Hungarian University of Agriculture and Life Sciences

Tribomechanics of 3D printed elements with variable material structure

DOI: 10.54598/003920

Thesis of the doctoral (PhD) dissertation

József Dobos

Gödöllő - Hungary
2023

Doctoral school denomination:	Doctoral School of Mechanical Engineering
Science:	Mechanical Engineering
Head of school:	Prof. Dr. Gábor Kalácska, DSc Institute of Technology Hungarian University of Agriculture and Life Sciences, Gödöllő - Hungary
Supervisors:	Dr. Róbert Zsolt Keresztes, PhD Institute of Technology Hungarian University of Agriculture and Life Sciences, Gödöllő - Hungary Dr. István Oldal Institute of Technology Hungarian University of Agriculture and Life Sciences, Gödöllő - Hungary

.....

....

Affirmation of supervisors Affirmation of head of school

CONTENTS

1. INTRODUCTION, OBJECTIVES

1.1. Objectives

The aim of my research is to optimize the filling (material consumption) of 3D printed plastic parts. The technology allows for parts within a part to have different infill levels and gives the possibility to reduce the infill and thus the amount of material used in certain places, based on the knowledge of the loads. This has two advantages in production; firstly, it reduces the amount of material used, secondly, it reduces production time and both are cost saving factors.

My research is mainly about the optimal design of layers with different patterns by varying the density and size of the layers. Using simulations, I want to illustrate the search for the optimum of pairing different printing patterns. The expected results will be illustrated using different infills and printing patterns.

In order to achieve these objectives, I will set out the following subtasks:

- Experimental studies on the determination of tensile strength and elastic modulus using different infill density and pattern pairs. The results are used as input parameters to construct a working mechanical model based on accurate and realistic material properties.
- Virtual mechanical analysis of sandwich specimens using finite element method. This is used to determine the optimum thickness with the highest specific load (sandwich core) for given loading patterns and densities.
- Simulation of a multi-layered machine component to determine the contact mechanical properties and to find the optimum layer arrangement/settings.
- Testing of the obtained results on machine components, tribological tests, validation of the obtained finite element results.

1.2. Mechanical test

PLA (Polylactic acid) was used in my measurements. This environmentally conscious raw material is produced from plants with a high starch content (wheat, maize and rice). The manufactured workpieces were perfectly suitable for capturing without any post-processing, thus allowing tensile strength and elastic modulus tests. The internal structure of the standard 3D printed specimens made according to ISO 527 is illustrated in Figure 2.1. The specimens were fabricated with printing settings of internal structure/pattern named concentric, Hilbert curve, honeycomb and rectilinear. The settings allow to change the fill rate (percentage) and pattern of the material usage. The four types of pattern are further grouped into four different infill levels: 40%, 60%, 80% and 100%, creating a comparison of 15 variations.

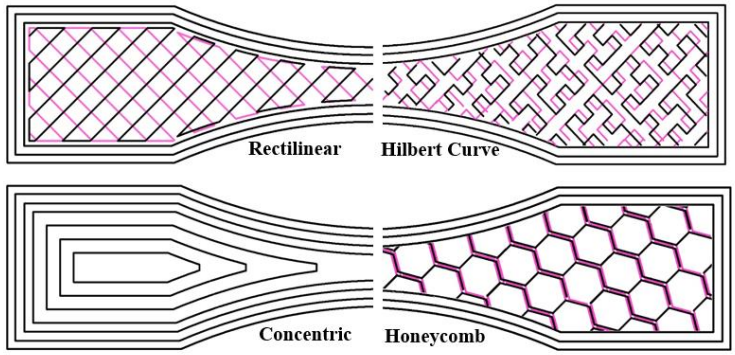

Figure 2.1 Internal structure patterns of ISO 527 specimens

For the elastic modulus measurements, I printed one copy of each of the patterns and fills used above. The Young-modulus measurements can be easily reproduced on the same test specimen, eliminating the need to re-produce 15 variations.

1.3. Virtual model testing of a bent sandwich structure

The aim of virtual model tests is to find the optimal layering of three-layer 3D printed elements with different patterns and fillings. My research presented above has provided the basis for creating a working mechanical model based on accurate and realistic material properties. Subsequently, I started a series of virtual bending tests on an ISO-178 standard sandwich structure specimen using Ansys Workbench software. The tests were used to determine the optimum ratio of sandwich core to shell for the element with the highest specific load capacity for the given loading patterns and infill. I modeled in

static, i.e., at rest, since the speed of the tensile test does not require dynamic modelling. Since the cross-section is constant, and the type of standard test allows it, I modeled the material in two dimensions, so I can get results with the same accuracy much faster. I have designed the specimen used in the finite element method taking into account the ISO 178 standard shown in Figure 2.2. Based on this picture, I created the additional boundary conditions to run the program to determine the maximum stress. The dimensions of the standard specimen are shown in the following figure. Length 80 mm, width 10 mm and specimen thickness 4 mm.

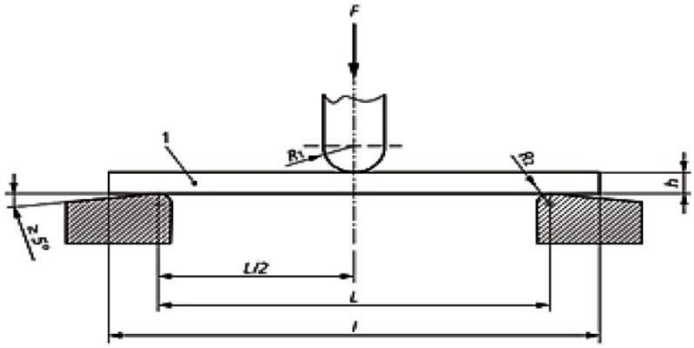

Figure 2.2. ISO 178 bending test representation

The specimen was tested by varying the layers, patterns and fills from measurement to measurement, the same as in the previous settings. That is, in the experiment, the shell layer was tested in all cases with 100% and rectilinear patterns, and the inner layers were tested based on the previous ones; concentric, rectilinear, honeycomb, Hilbert curve and in 40, 60, 80 and 100% fill variations. In accordance with ISO 178, the height of the specimen is constant at 4 mm throughout the test. The purpose of the modelling is to determine the effect of varying the filling of the internal structure on the properties of the test specimen. The test was performed using standard two-support three-point bending, as illustrated in Figure 2.1. Taking advantage of the symmetry, it is sufficient to model half of the real geometry in the virtual test. One half of the test specimen was supported, and the other end was loaded with force F to form the test model. A caster support was thus placed on the end as a boundary condition, and a force was placed in the middle, in the plane of symmetry. And the symmetry boundary condition was implemented so that the horizontal displacement in the middle - on the axis of symmetry - is zero. The test method of the ISO 178 bending standard and the mesh of the finite element model are shown in Figure 2.3. The finite element mesh contains 6480 nodes and 2069 elements.

The mesh elements are rectangular in shape between 0.05 and 0.5 mm. Their size is smallest at the critical part, i.e. around the maximum stress, and increases away from this point. The support is modelled as a y-displacement, with half the force applied for symmetry. I modelled the symmetry as displacement in the x = 0 plane.

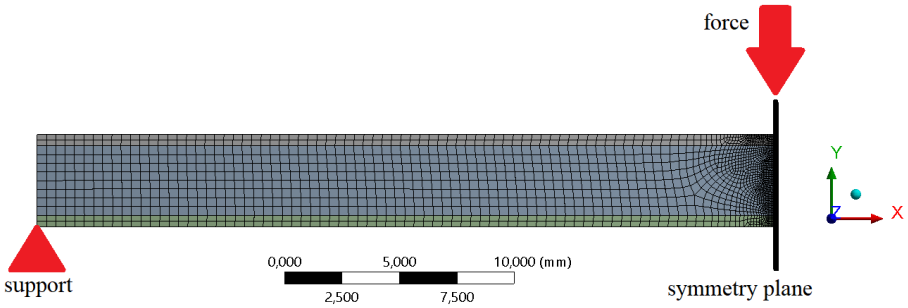

Figure 2.3 The sandwich structure model mesh

1.4. Finite element model tests for machine elements

An important consideration in the choice of the machine element was its ease of use in tribological tests to validate the results. The test bench in the MATE Tribology laboratory is well suited for testing disc with a diameter of 60 mm and therefore the test rig shown in Figure 2.4 was designed. The disc was designed in Solid Edge software.

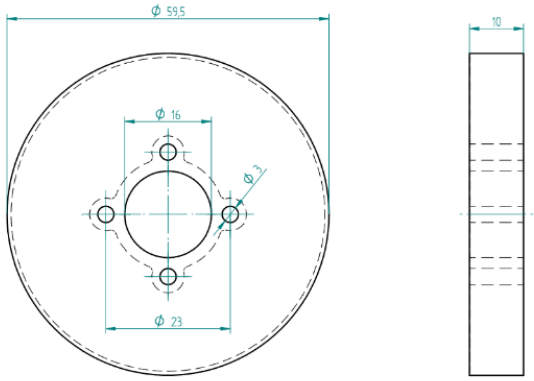

Figure 2.4 Geometric dimensions of the tested PLA disc

The cross-section constancy and the standard test type allow two-dimensional modelling. These settings allowed me to obtain results with the same accuracy much faster. As before, the shell structure is 100% rectilinear in all cases. For the bending tests, I investigate the 40% infill that produces

the best results, varying concentric, Hilbert curve, honeycomb and rectilienar patterns. The shell thickness I tested four different samples with 40 percent filling, varying seven core thicknesses, for normal stress, reduced stress and deformation component values. The purpose of the modelling was to find the shell thickness above which it is unnecessary to add additional material to the machine component. The shell thicknesses used in the tests were 0.5; 1; 1.5; 2; 3; 4 and 5 mm. The discs illustrated in Figure 2.4 was used in the test. The disc was supported and guided as shown in Figure 2.6. The test model was developed using the test load applied previously. The disc under test was loaded with the supports and forces shown in Figure 2.2.2. The fixed support shows the support, and the displacement shows the guiding to stabilize the discs. In a first step, I compressed the machine elements by 0.002 mm to make the model numerically stable. In the second step, I released the compression and compressed the discs by force. A load of 50 N was applied during the tests.

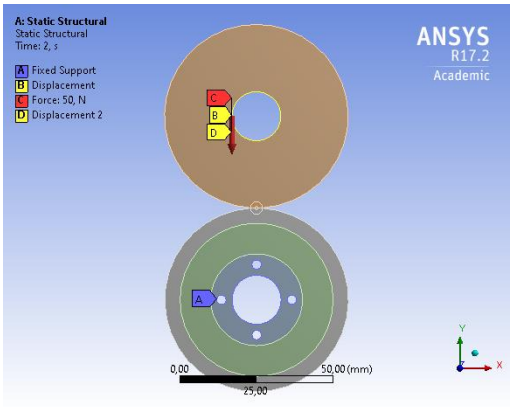

Figure 2.6. Applied supports and forces

The finite element mesh contains 4,832 nodes and 1,464 elements. The mesh elements are rectangular in shape between 0.05 and 0.5 mm. Their size is smallest at the critical part, i.e. around the contact point. Near the contact surfaces, the variation of stress is the largest, which can be followed by the small element size, the mesh size increases away from the critical point.

1.5. Tribological tests

The results obtained from the tensile and elasticity tests provided the input parameters for the virtual test series. To verify and validate these results, tribological analysis on machine components were the next step of my studies. The twin disc test bench used for the tests was developed by the MATE Technical Institute. Its operating principle is almost identical to the twin disc system. The test rig allows wear or even fatigue testing of machine components under near constant load (Figure 2.7).

2.7. The test rig (using the twin disc principle)

The test rig (or test bench) was built in a similar way to the Twin-Disc systems. An electric motor-driven closed drive train with adjustable frequency converter is responsible for providing speeds from 0 to 1500 rpm. The electric motor only compensates for drive losses, making the system very economical to operate. During the test, the desired load can be created between the discs by means of weights fixed to the drive. The weight/load was determined using a load cell calibrated in the Catman program. The data were processed and saved using Catman software. When the motor is switched on, two parallel shafts are driven by means of a ribbed belt drive. The parallel shaft associated with the tension belt is connected to the driving, tested disc. The centre of this shaft is fitted with a torque sensor and the other end of the shaft is located in the drive. The Spider 8 type measuring amplifier provides the information to the Catman software by processing the data and monitoring it in real time. The belt rotates the driven discs, which are connected to the other parallel shaft through the drive gear.

The four test parameters are measured continuously using Catman software, HBM Spider 8 and a Calex PCCFMT-O-3M temperature sensor for simultaneous measurement data acquisition. The recorded parameters are: speed, friction torque, time and the temperature of the disc surface. Input parameters affecting the test result; size, material, structure, filling of the drive and driven discs. To measure the torque, a torque sensor placed in the centre of the drive shaft mentioned earlier was used. The measuring frequency was 2 Hz in all cases. The data series were saved in Catman proprietary format, which I processed in Microsoft Excel.

3. RESULTS

In the following, I present my new scientific results from my research. The resulting diagrams are illustrated with the diagrams that are essential for clarity.

1.6. Results of the finite element method

Evaluation of simulation bending test results

Based on the boundary conditions and settings used, 225 cases were modelled. Stress values were documented for all fillings and material pattern variations. From the calculated stresses, I determined the ultimate tensile strength values to which the specimen could be loaded. I obtained the calculated force values as a function of the change in ply thickness. The core and shell do not fail at the same load due to different material properties. For both layers, the maximum load on the layer must be determined and the smaller of the two must be taken into account in the evaluation as the ultimate load of the structure. Calculating with the smallest values - which the material can certainly withstand - and the mass of the specimens, I obtain the mass-force ratio, which shows the specific load capacity as a function of the infill. Plotting these results in a graph, the curve of the function shows an extreme value, i.e. it has an optimum.

The evolution of the specific load under varying core thickness is illustrated in Figures 2.7 a-d. The optimum core thickness was tested with all previously applied settings (varying charge density and pattern). The vertical axis of the diagrams shows the value of the force to mass ratio and the horizontal axis shows the material thickness of the internal structure. Also, for the Hilbert curve patterns, the values for 40% fill are excellent, with the optimum at 1.8 mm.

For the honeycomb patterns, the difference between the functions is getting smaller and smaller, and for the rectilinear patterns there is little or no significant difference. Again, the highest specific load capacity is obtained at 40% infill and 1.8 mm material thickness. When examining specimens with 100% infill, it can be seen that there is no optimum curve, the function is almost flat. The main reason for this is that the shell sandwich layers have the same infill (100%).

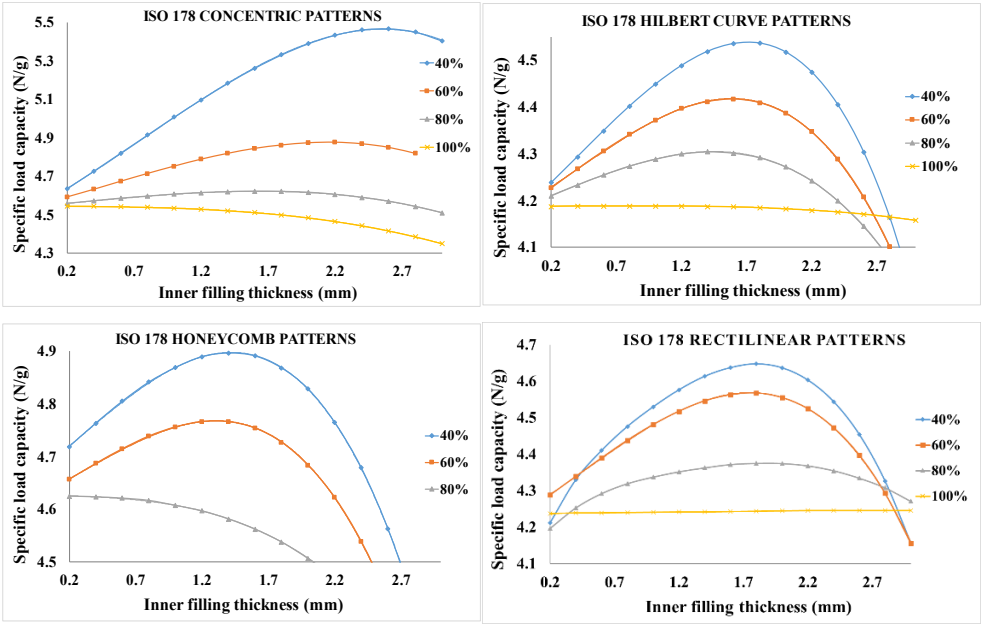

Figures 2.7 a-d Variation of specific load capacity as a function of inner core thickness (a) concentric, (b) Hilbert curve, (c) honeycomb, and (d) rectilinear pattern.

Therefore, the material properties did not improve despite the increasing core thickness. This was more apparent in the rectilinear sample, where the trend line was relatively straight as the shell and core pattern and fill ratio were the same. The fact that there is always a significant drop off after the peak of the specific load curve, especially at 40 and 60% fill, clearly shows the importance of the optimum. The optimum does not seem to be related to a given thickness in all circumstances. In summary, it is clear from the diagrams that an optimum exists using infill density and patterns. Thus, it can be concluded that for a three-layer printed sandwich structure, there exists an optimal layer thickness ratio in terms of load-bearing capacity for all fillings and patterns. The assumption for the existence of the optimum is that the load capacity of the shell layer is greater than the load capacity of the core, but the density of the inner infill is less.

It can be clearly seen that the best specific load capacity is always observed at 40% infill density, regardless of the infill pattern.

Evaluation of simulation machine element test results

Based on my calculations and the 3D printing parameters (sample and variation of the filling density), I investigated the stresses and deformations on the shell structure of a sandwich disc. Normal stress, equivalent stress (reduced stress) and directional deformation (horizontal) component values were documented for all fillings and material pattern variations. Based on the applied boundary conditions and settings, 315 results were obtained. An illustration of the normal stress for the 40% specimens is shown in Figure 2.8. results. The normal stress includes only the values of the compressive force perpendicular to the surface. The vertical axis of the above diagram shows the calculated stress and the horizontal axis the value of the shell thickness. At 2 mm, the normal stress is almost constant. The points are well fitted by the saturation curve describing the phenomenon (marked in blue), which is illustrated in Figure 2.8.

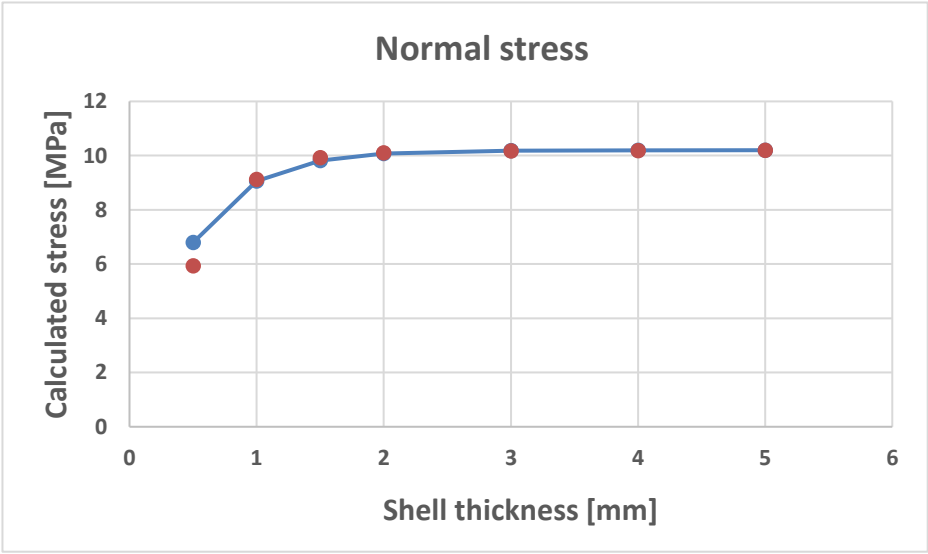

Figure 2.8. Calculated normal stress as a function of shell thickness and the fitted curve

The equation of the function shown in the figure:

$f(x) = c_1 \cdot (1 - e^{-c_2 x})$

where the constants after the fit are: c_1=10,2, c_2=2,2.

Based on the fitted function, a limit can be determined above which increasing the layer thickness has negligible effect on the tribological local conditions. The c_1 indicates the limit value of the function.

If we accept a deviation of 5%, we can consider the function to be constant from 95% of this, at which point:

$0{,}95=1-e^{-2{,}2x}$

from this: $x=\frac{\ln 0{,}05}{-2{,}2}$= 1,36 mm.

If 1% of the deviation is acceptable, then 99% of the value of the function can be considered constant;

$x=\frac{\ln 0{,}01}{-2{,}2}$= 2,09 mm.

From this for a 5% approximation, a shell thickness of 1.36 mm, for 1% 2.09 mm is the limit above which it is not worth increasing the layer any further, because it does not cause any improvement in local mechanical properties. The values of the deformation component are the amount of deformation in the x direction of displacement (slip), i.e. the values of the curve of the function are also constant at a shell thickness of 2 mm. No significant difference is observed between the two patterns, the curves of the functions showing almost the same trend. The steady state of stresses in all conditions and patterns is related to a given thickness. In summary; when evaluating the plots, I observed that the range of results of the functions can be divided into two parts. For the variable values, it can be said that the layer thickness has an effect on the stresses and deformations. In the other half of the range, however, it is observed that the layer thickness has negligibly little effect on stress and deformation. As a consequence, it can be concluded that there is a limit above which it is no longer worth increasing the shell thickness because in practice it will have no effect on the tribological properties.

Therefore (thesis) the stress values as a function of shell thickness can be approximated well by a saturation function. Furthermore, (thesis) there is a limit above which increasing the shell thickness has negligible effect on tribological local conditions.

1.7. Results of tribological tests

In the following, I will turn to the presentation of the tribological measurement results that validated the finite element method. The tribological model tests on the disc were carried out to validate the simulation results obtained in the finite element. It is important to note that the tests were performed at ambient temperature and under normal humidity conditions. The shell thickness of the PLA discs was 1 mm, 2 mm, 4 mm and the counter disc was steel in all cases. The detailed properties of the materials used are described in the material and method section. During the tests, I continuously measured the drive torque loss and the polymer disc surface temperature. The temperature measurement point is illustrated in Figure 2.9.

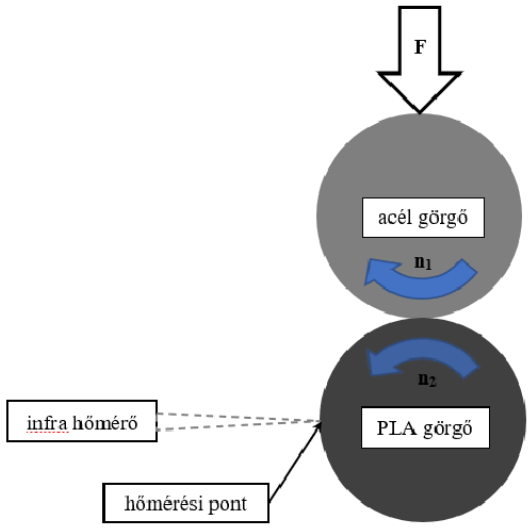

Figure 2.9. Measuring the temperature of discs

From the measured data I created a complex diagram showing the temperature and torque loss as a function of time. I have marked the values for different shell thicknesses in different colours. The upper part of the diagram shows the temperature rise (T [°C]) and the lower part the torque loss (M [Nm]). From the measurement diagram it is obvious that there is no significant difference in the temperature variation depending on the shell thickness. This can be explained by the location of the temperature measurement point. Of course, the temperature measurement should have been carried out in the contact zone, but this was not possible. The torque loss curves showed much larger deviations in agreement with the finite element simulation results. It is very clear that the 1 mm shell thickness disc differs greatly from the torque loss measured on the 2 mm and 4 mm shell thickness discs.

However, as the finite element tests have preliminarily confirmed, which has also been shown in the tribological tests, there is no longer a significant difference between the results of 2 mm and 4 mm shell thickness discs. Figure 2.10 illustrates the measurement diagram of these results.

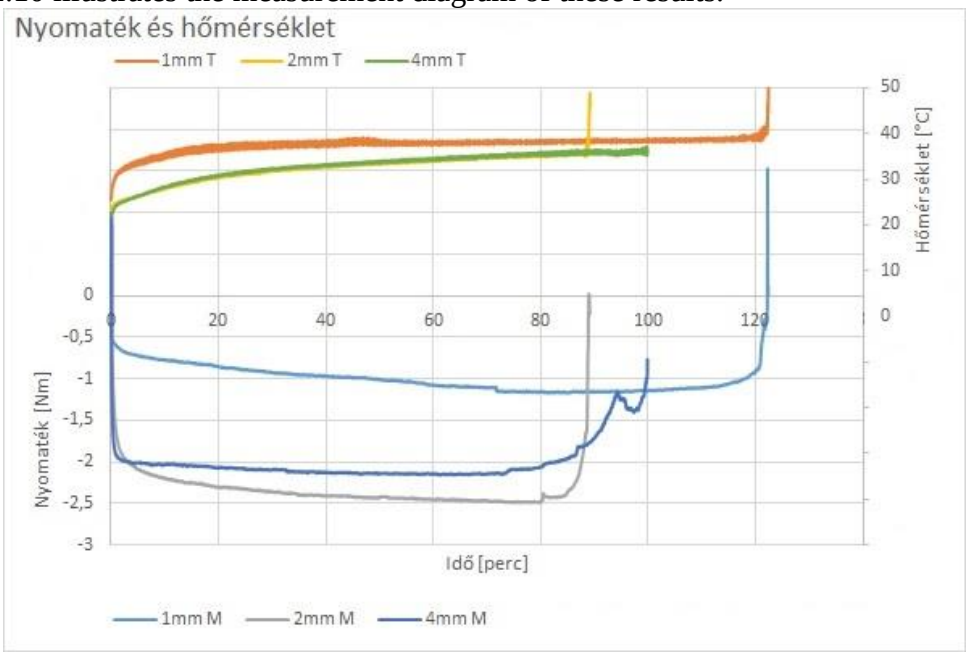

Figure 2.10. Twin disc test measurement diagram for different shell thicknesses

Ont he basis of the results illustrated in the diagram, I can demonstrate the validity of the results obtained by the finite element simulation method.

4. NEW SCIENTIFIC RESULTS

Thesis 1.

For a three-layered, 3D printed, curved sandwich structure, there is an optimum layer thickness ratio for each fill and pattern in terms of specific load capacity. The assumption for the existence of an optimum is that the shell layer has a higher load carrying capacity and infill percentage than the core material (in 3D printing, this is always met by reducing the core filling). A thinner or thicker shell than the optimum thickness will also result in a lower specific load capacity.

Thesis 2.

For a three-layered, 3D printed, curved sandwich structure, the best specific load capacity is always achieved at 40% core infill, regardless of the filling pattern.
For the PLA base material and infill pattern used in the study, there is an optimum specific load capacity. The values for the infill pattern and core thickness are as follows:

Filling density	Optimum values for inner core thickness							
	concentric		**Hilbert curve**		**honeycomb**		**rectilinear**	
	Optimum core thickness (total thickness 4 mm)							
	mm	%	mm	%	mm	%	mm	%
40 %	2.6	65	1.8	45	1.6	40	2	50
60 %	2.2	55	1.6	40	1.4	35	2	50
80 %	1.6	40	1.5	37.5	0.2	5	2	50

Thesis 3.

Based on a theoretical strength study of a three-layered, 3D printed, PLA disc, I found that the stress values in the immediate vicinity of the contact can be well approximated by a so-called saturation function as a function of shell thickness. The shell is 100% filled in all cases, the inner layer is less filled.
The general equation of the function is:

$$f(x) = c_1 \cdot (1 - e^{-c_2 x})$$

where:

- x: thickness of the shell,
- c_1 and c_2 are constants (material, geometry and load dependent).

Thesis 4.

In the case of a three-layered, 3D printed, PLA disc, there is a limit to the shell thickness, which, when increased, does not significantly change the local tribological conditions.
The theoretical limit was established using the function described in Thesis 3 for a steel-PLA disc pair with a diameter of 60 mm and a load of 50 N. Then the constants of the function are: c_1=10.2, c_2=2.2.

For a 5% error margin of 1.36 mm and a 1% error margin of 2.09 mm shell thickness is the limit above which it is not worth increasing the shell thickness, because it does not cause any further improvement in local mechanical properties.
This was verified by tribological testing of PLA discs with 1 mm, 2 mm, and 4 mm shell thickness. The 1 mm shell is below the limit, the 2 mm and 4 mm shells are in the constant section.

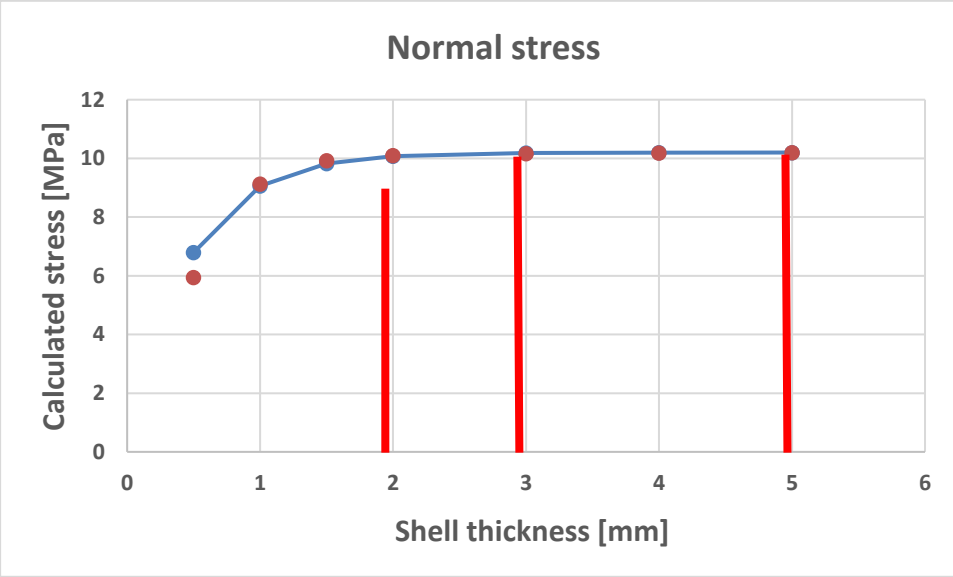

From the measurement results, it was clear that the measured characteristics of the 2 mm and 4 mm shell thickness discs are almost the same, while they are different for the 1 mm shell. Thus, the existence of a steady-state phase established from the theoretical saturation curve was confirmed by practical tests.

5. CONCLUSION AND SUGGESTIONS

In the literature, there are many good results for improving the load capacity of a structure by varying the infill of 3D printing. However, these are typically specific solutions, or procedures, that can be applied to a particular structure. In fact, some researchers do not consider the general results feasible. In contrast, in my thesis I have managed to obtain some generalisable results that are valid under certain (and most of the time in practice) circumstances. I have conducted research and obtained results in two different areas, both similar in the technology, materials and methods used. The first area is the bending of printed polymer sandwich structures, the second is the tribology of multilayer printed polymer discs.

My hypothesis in both areas was that optimum thicknesses of the layers exist, but I had to prove the existence of the optimum under completely different boundary conditions. I summarised my conclusions based on my research work in four theses, which I have explained in detail in the previous chapter. In addition, I have drawn some conclusions throughout the work:

- If we look in the right area, generalised results can be obtained for 3D printed bodies. In my case, this was a three-layer sandwich structure and a three-layer disc, with enough conditions to satisfy that both the infill and strength of the inner structure were less than that of the outer layer, which in practice is almost always satisfied.

- Tribological properties and behaviour are correlated with contact mechanical properties even if otherwise identical tribological boundary conditions are not applied, but the loads and mechanical properties are accurate.

- In the future, by including slip, sliding velocities, wear, further matches or even limits of applicability could be established with the static contact model.

- It is worthwhile to extend further investigations to the use of nonlinear material models in VEM simulations. Based on my results, the linear model was sufficiently accurate, however, investigating the improvement of a nonlinear model is an interesting future task.

6. SUMMARY

The applicability and growing use of 3D printed products is now significant in manufacturing applications. In a manufacturing technology that is new to the industry, it is important to clarify the possibility of expected anomalies, possible failures, loss of use. The advantages over subtractive manufacturing lie mainly in environmentally conscious, manufacturing efficiency and ease of material structure modification. The main advantages of inhomogeneity and uniformity of scaling within the material structure that can be achieved by 3D printing are structural optimization. The internal structure of the fabrication is not uniformly load distributed, so it is possible to reduce the material density in the lower load area. Through my research, simulation studies and 3D printing experiments, I have produced results that contribute to the development of additive manufacturing.

In the first part of my thesis, I investigated the mechanical properties of a printed sandwich structure. The infill pattern has an effect on the mechanical strength and the specific load capacity. Among the settings, I investigated the influence of shell thickness and core thickness. The results obtained from the mechanical tests were used as input parameters for the simulation software.

This allowed me to perform the simulation process of the bending test with real input material properties.
I found that the simulation results of the PLA body with sandwich structure that I set up showed that the highest specific load capacity was observed at 40% fill density in all cases, regardless of the fill pattern.
It is also found that for a three-layer printed sandwich structure, there exists an optimal layer thickness ratio for each fill and pattern in terms of specific load carrying capacity. The assumption for the existence of an optimum is that the load carrying capacity of the shell layer is greater than that of the core, but the density of the inner infill is less.
It is found that for a two-layered machine element, there exists a limit to the shell thickness, which, if further increased, does not significantly change the tribological local conditions. Using a thicker shell does not improve the tribological properties but increases the weight of the part and the printing time and cost.
I also evaluated the surface roughness and microscopic surface photographs of the discs in terms of their correlation with tribological behavior, which supported the applicability of the results of the mechanical simulations in terms of wear.
In the course of my research, I have found that the field of three-dimensional printing and tribology of polymers and composites still has many new and unexploited areas.
The applicability and growing use of 3D printed products is now significant in manufacturing applications. In a manufacturing technology that is new to the industry, it is important to clarify the possibility of expected anomalies, possible failures and loss of use. The advantages over subtractive manufacturing lie mainly in environmentally conscious, manufacturing efficiency and ease of material structure modification. The main advantages of inhomogeneity and uniformity of scaling within the material structure that can be achieved by 3D printing are structural optimization. The internal structure of the fabrication is not uniformly load distributed, so it is possible to reduce the material density in the lower load area.
My research has produced results from simulation studies and 3D printing experiments that provide useful information for engineering practice.

7. PUBLICATIONS

1. **Dobos, J.;** Keresztes, R. Oldal, I.; 3D nyomtatott szendvicsszerkezetű görgők tribológiai hajtásvizsgálata, Mezőgazdasági Technika (megjelenés alatt)
2. Kári-Horváth, A. ; Pataki, T. I. ; **Dobos, J**. ; Szilágyi, N., Ultrahangos fémhegesztés bemutatása, Mezőgazdasági Technika 63 : 7 pp. 18-20., 3 p. (2022)
3. **Dobos J.**, Hanon M. M., Oldal I. (2021): Effect of infill density and pattern on the specific load capacity of FDM 3D-printed PLA multilayer sandwich. Journal of Polymer Engineering, De Gruyter. ISSN: 0334-6447, https://doi.org/10.1515/polyeng-2021-0223, (2021)
4. H., Muammel M. ; **Dobos, J.** ; Zsidai, L., The influence of 3D printing process parameters on the mechanical performance of PLA polymer and its correlation with hardness, Procedia Manufacturing 54 pp. 244-249., 6 p. (2021)
5. Hanon M. M., **Dobos J.**, Zsidai L. (2021): The influence of 3D printing process parameters on the mechanical performance of PLA polymer and its correlation with hardness. 10th CIRP Sponsored Conference on Digital Enterprise Technologies (DET 2020), Budapest, Hungary, October 11–13, 2021. Published in: Procedia Manufacturing, Elsevier. 54, 244249. ISSN: 2351-9789
6. **Dobos J.,** Keresztes R.; Abrasive wear of filled polymer composites: A brief review. In: Magó, László; Kurják, Zoltán (szerk.) SYNERGY - Engineering, Agriculture and Green Industry Innovation : PAPERS of the VI. International Conference of CIGR Hungarian National Committee and the Szent István University, Faculty of Mechanical Engineering and the XXXIX. R&D Conference of Hungarian Academy of Sciences, Committee of Agricultural and Biosystems Engineering Gödöllő, Hungary, 4 – 6. November 2019 (Electronical issue). Gödöllő, Magyarország: Szent István University Faculty of Mechanical Engineering (2019) Paper: N6-4-212, 6 p.
7. Kiss, P ; Hajdú, J ; Máthé, L ; Dobos, J. ; Magó, L Vontatott mezőgazdasági járművek, munkagépek európai gyártóinak és piacának felmérése. Mezőgazdasági Technika, 59: 3 pp. 1-5., 5 p. (2018)
8. Pillinger, Gy. ; Máthé, L. ; **Dobos, J.** ; Kiss, P., Pressure regulation in pneumatic tractor tyres. Mechanical Engineering Letters: R and D: Research and Development 17 pp. 91-97., 7 p. (2018)

9. Kiss, P. ; Hajdú, J. ; Máthé, L. ; **Dobos, J.** ; Magó, L.; Analysis of the towed agricultural machinery manufacturers in Europe, Hungarian Agricultural Engineering: 33 pp. 1-7., 7 p. (2018)
10. Kiss, P. ; Hajdú, J. ; Máthé, L. ; **Dobos, J.** ; Magó, L. Analysis of the towed agricultural machinery manufacturers in Europe, Hungarian Agricultural Engineering: 33 pp. 5-10., 6 p. (2018)